

# A deterministic map of Waddington's epigenetic landscape for cell fate specification

Bhattacharya *et al.*

RESEARCH ARTICLE

Open Access

# A deterministic map of Waddington's epigenetic landscape for cell fate specification

Sudin Bhattacharya\*, Qiang Zhang and Melvin E Andersen

## Abstract

**Background:** The image of the “epigenetic landscape”, with a series of branching valleys and ridges depicting stable cellular states and the barriers between those states, has been a popular visual metaphor for cell lineage specification - especially in light of the recent discovery that terminally differentiated adult cells can be reprogrammed into pluripotent stem cells or into alternative cell lineages. However the question of whether the epigenetic landscape can be mapped out quantitatively to provide a predictive model of cellular differentiation remains largely unanswered.

**Results:** Here we derive a simple deterministic path-integral quasi-potential, based on the kinetic parameters of a gene network regulating cell fate, and show that this quantity is minimized along a temporal trajectory in the state space of the gene network, thus providing a marker of directionality for cell differentiation processes. We then use the derived quasi-potential as a measure of “elevation” to quantitatively map the epigenetic landscape, on which trajectories flow “downhill” from any location. Stochastic simulations confirm that the elevation of this computed landscape correlates to the likelihood of occurrence of particular cell fates, with well-populated low-lying “valleys” representing stable cellular states and higher “ridges” acting as barriers to transitions between the stable states.

**Conclusions:** This quantitative map of the epigenetic landscape underlying cell fate choice provides mechanistic insights into the “forces” that direct cellular differentiation in the context of physiological development, as well as during artificially induced cell lineage reprogramming. Our generalized approach to mapping the landscape is applicable to non-gradient gene regulatory systems for which an analytical potential function cannot be derived, and also to high-dimensional gene networks. Rigorous quantification of the gene regulatory circuits that govern cell lineage choice and subsequent mapping of the epigenetic landscape can potentially help identify optimal routes of cell fate reprogramming.

## Background

The biologist Conrad Hal Waddington, in the course of a career spanning four decades (1930s - 1970s), attempted a bold synthesis of the fields of genetics, embryology and evolution [1,2]. The centerpiece of his vision was the idea of the “epigenetic landscape”, first described in *An Introduction to Modern Genetics* [3], and elaborated in subsequent monographs [4,5]. Waddington portrayed the epigenetic landscape as an inclined surface with a cascade of branching ridges and valleys (Figure 1A), which in the context of cell lineage selection, represent the series of “either/or” fate choices made by a developing cell. He envisioned that on this

landscape, “the presence or absence of particular genes acts by determining which path shall be followed from a certain point of divergence [1,4]”, thus providing in a single image an appealing, and influential, metaphor for the connection between genotype and phenotype.

In the quantitative view of a cell as a dynamical system governed by genetic interaction networks [6], an intuitive association can be made between the valleys (“creodes” in Waddington's terminology) on the epigenetic landscape and the trajectories leading to the *attractors*, or stable steady states, of the gene networks that regulate cell fate [7-9]. But can we quantitatively map the undulating surface of the landscape, thereby providing a predictive model of the “directionality” of cellular differentiation? Waddington himself cautioned that the epigenetic landscape, while useful as a “rough

\* Correspondence: sbhattacharya@thehamner.org  
Division of Computational Biology, Program in Chemical Safety Sciences, The Hamner Institutes for Health Sciences, Research Triangle Park, NC 27709, USA

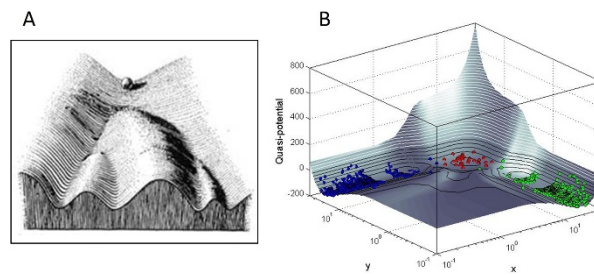


**Figure 1 Mapping Waddington's epigenetic landscape.** (A) The “epigenetic landscape” proposed by Conrad Waddington shows a ball rolling down valleys separated by ridges on an inclined surface, as a visual metaphor for the branching pathways of cell fate determination. Figure reproduced from original text by Waddington [5]. (B) The computed epigenetic landscape for a two-gene ( $x$  and  $y$ ) regulatory network with mutual inhibition and positive autoregulation, where the elevation represents a path-integral quasi-potential derived from the deterministic rate equations describing the interactions of the two genes. We show that the “valleys” on this computed surface correspond to stable steady states (attractors) of the network, while the “ridges” separating the valleys represent barriers to stochastic transitions among multiple steady states. Colored circles represent a population of stochastically simulated “cells” (multiple instances of the network) residing in different stable steady states.

and ready picture” of development, “cannot be interpreted rigorously [5]”. The mathematician René Thom, in his formulation of *catastrophe theory* inspired by Waddington's ideas, proposed that a generalized “potential surface” could be derived for any dynamical system [2,10]. However Thom's later writings suggest that he did not believe it possible to quantify the epigenetic landscape [11]. This view has been echoed by other authors, who have described the landscape as a “colorful metaphor [2]” with “no grounding in physical reality [1]”.

Huang, Wang and colleagues have recently proposed a probabilistic “pseudo-potential” to quantify the epigenetic landscape for a gene network regulating cell fate, where the elevation of the surface is inversely related to the likelihood of occurrence of a particular state in phase space [8,12,13]. In this formulation a stochastic potential energy landscape is characterized for a gene network, based on a Hartree mean-field approximation of the underlying master equation [14]. Such stochastic formulations have also been used to derive probabilistic potential landscapes for the lysis-lysogeny switch in bacteriophage lambda [15-17], the mitogen-activated protein kinase (MAPK) signal transduction network [18], biochemical oscillations [19], and the predator-prey system [20].

Here we propose a simple numerical method to map the epigenetic landscape that is not based on a probabilistic or master-equation approach. Instead, a quasi-potential surface (Figure 1B) is derived directly from the deterministic rate equations governing the dynamic behavior of a gene regulatory circuit. We then use stochastic simulations to show that the elevation of this computed landscape correlates to the likelihood of occurrence of particular cell fates, with well-populated low-lying valleys representing stable cellular states and

higher ridges acting as barriers to transitions between the stable states.

Finally, we discuss ways in which this quantitatively mapped landscape may help predict the efficiency of cellular de-differentiation or trans-differentiation, and identify optimal routes of cell fate reprogramming. Recent discoveries have challenged the dogma of cell fate determination as a unidirectional and irreversible process. Even terminally differentiated adult cells have now been shown to retain considerable phenotypic plasticity and the ability to be reprogrammed into pluripotent stem cell-like states [21-27] or into alternative differentiated lineages [28-34] by forced expression of a single gene or a small number of genes. These findings have led to a resurgence of interest in Waddington's ideas about cell lineage choice, with several authors invoking the image of the epigenetic landscape [7-9,35-39]. However the theoretical basis of plasticity in cell fate is still not fully understood, and the efficiency of reprogramming in these studies is often quite low [36]. A quantitative understanding of the “forces” that drive cell differentiation, and the “barriers” that separate stable cell states, is urgently needed. Such understanding may eventually enable us to predict the relative ease or difficulty of de-differentiation or trans-differentiation among multiple cellular states.

## Results and Discussion

### Derivation of the quasi-potential landscape

We first illustrate our quantitative approach with a simple circuit of two genes  $x$  and  $y$  that inhibit each other, forming a double-negative feedback loop structure (see **Methods**). This circuit works as a toggle switch with two stable steady states: one state with high  $y$  and low  $x$  expression, and the other state with high  $x$  and low  $y$  expression [40]. Such “bistable” switches formed by

mutual antagonism of a pair of key regulatory genes underlie many binary cell fate choices [7,13]. The circuit can be described as a two-variable dynamical system, with the rate of change in expression of each of the two genes given as a function of their expression levels:

$$\begin{aligned} \frac{dx}{dt} &= f(x, y) \\ \frac{dy}{dt} &= g(x, y) \end{aligned} \quad (1)$$

If we were able to derive a closed-form potential function  $V(x, y)$  for the system in Eq. 1 that satisfied the conditions:

$$\begin{aligned} \frac{\partial V}{\partial x} &= -\frac{dx}{dt} \\ \frac{\partial V}{\partial y} &= -\frac{dy}{dt} \end{aligned} \quad (2)$$

then the local minima on the two-variable potential surface  $V(x, y)$  would correspond mathematically to the stable steady states of the system, given that at the local minima on the surface ( $\partial V/\partial x = 0$ ;  $\partial V/\partial y = 0$ ), the rates of change in expression of both genes  $x$  and  $y$  would be zero (per Eq. 2). But such a closed-form potential function can be derived only in the case of a *gradient system*, defined by the condition [41]:

$$\frac{\partial f(x, y)}{\partial y} = \frac{\partial g(x, y)}{\partial x} \quad (3)$$

In general, condition (3) will not be valid for an arbitrary circuit of two genes  $x$  and  $y$  that regulate each other as per Eq. 1, making it impossible to derive a closed-form potential function.

Therefore, given that a gene circuit is in general a *non-gradient system*, we define a term  $V_q$  that changes incrementally along a trajectory followed by the system in  $x$ - $y$  phase space (Figure 2A) as follows:

$$\begin{aligned} \Delta V_q &= \frac{\partial V_q}{\partial x} \cdot \Delta x + \frac{\partial V_q}{\partial y} \cdot \Delta y \\ &= -\frac{dx}{dt} \cdot \Delta x - \frac{dy}{dt} \cdot \Delta y \end{aligned} \quad (4)$$

where  $\Delta x$  and  $\Delta y$  are sufficiently small increments along the trajectory such that  $\frac{dx}{dt}$  and  $\frac{dy}{dt}$  can be assumed to remain unchanged over the interval  $[(x, x+\Delta x); (y, y+\Delta y)]$ . The quantities  $\Delta x$  and  $\Delta y$  are obtained as the products  $\frac{dx}{dt} \cdot \Delta t$  and  $\frac{dy}{dt} \cdot \Delta t$ , respectively, where  $\Delta t$  is the time increment. We use the term “quasi-potential” to describe  $V_q$ , to emphasize its distinction from a closed-form potential function.

The change in the quasi-potential,  $\Delta V_q$ , can be rewritten from Eq. 4 as:

$$\begin{aligned} \Delta V_q &= -\frac{dx}{dt} \cdot \left( \frac{dx}{dt} \cdot \Delta t \right) - \frac{dy}{dt} \cdot \left( \frac{dy}{dt} \cdot \Delta t \right) \\ &= - \left[ \left( \frac{dx}{dt} \right)^2 + \left( \frac{dy}{dt} \right)^2 \right] \cdot \Delta t \end{aligned} \quad (5)$$

For positive increments in time  $\Delta t$ ,  $\Delta V_q$  is thus always negative along an evolving trajectory, ensuring that trajectories flow “downhill” along a putative “quasi-potential surface”. Stable steady states of the system ( $dx/dt = 0$ ;  $dy/dt = 0$ ) would correspond to local minima on this quasi-potential surface, given that at these states  $\Delta V_q = 0$  (per Eq. 5). The overall change in the quasi-potential along a trajectory can then be calculated by numerically integrating the quantity  $\Delta V_q$  in Eq. 4 from a given initial configuration up to a stable steady state, thereby allowing us to map out a temporal trajectory along the putative quasi-potential surface (Figure 2B). The quasi-potential thus defined is a measurable quantity that is minimized along a trajectory from any initial condition to an attractor in the phase space of the two genes, and is in effect a Liapunov function of the dynamical system represented by the two-gene circuit [41].

The procedure described above was repeated to evaluate the change in the quasi-potential along trajectories originating from different points in  $x$ - $y$  phase space. To derive a quasi-potential surface from multiple trajectories, we then make the following assumptions: (i) two trajectories with different initial conditions that converge to the same steady state must also converge to the same final quasi-potential level (Figure 2B); (ii) two trajectories that originate from “adjacent” initial conditions that are sufficiently close in  $x$ - $y$  phase space, but converge to different steady states, must start from the same initial quasi-potential level (Figure 2C). Observation (i) allows us to map out a basin of attraction from multiple trajectories converging to a single steady state; while observation (ii) enables the alignment of two adjacent basins of attraction along their shared basin boundary, or *separatrix*. (Essentially, (i) and (ii) together amount to the assumption that the putative epigenetic landscape is continuous.) The quasi-potential surface can then be obtained by interpolation among the aligned trajectories (Figure 2D, E), yielding the epigenetic landscape with its characteristic ridges and valleys (Figure 3A, B).

The same procedure can be applied to systems with more than two stable steady states - for instance, a “tristable” system produced by a circuit of two genes that induce their own expression, in addition to mutual inhibition (Figure 3C, D). This system has three steady

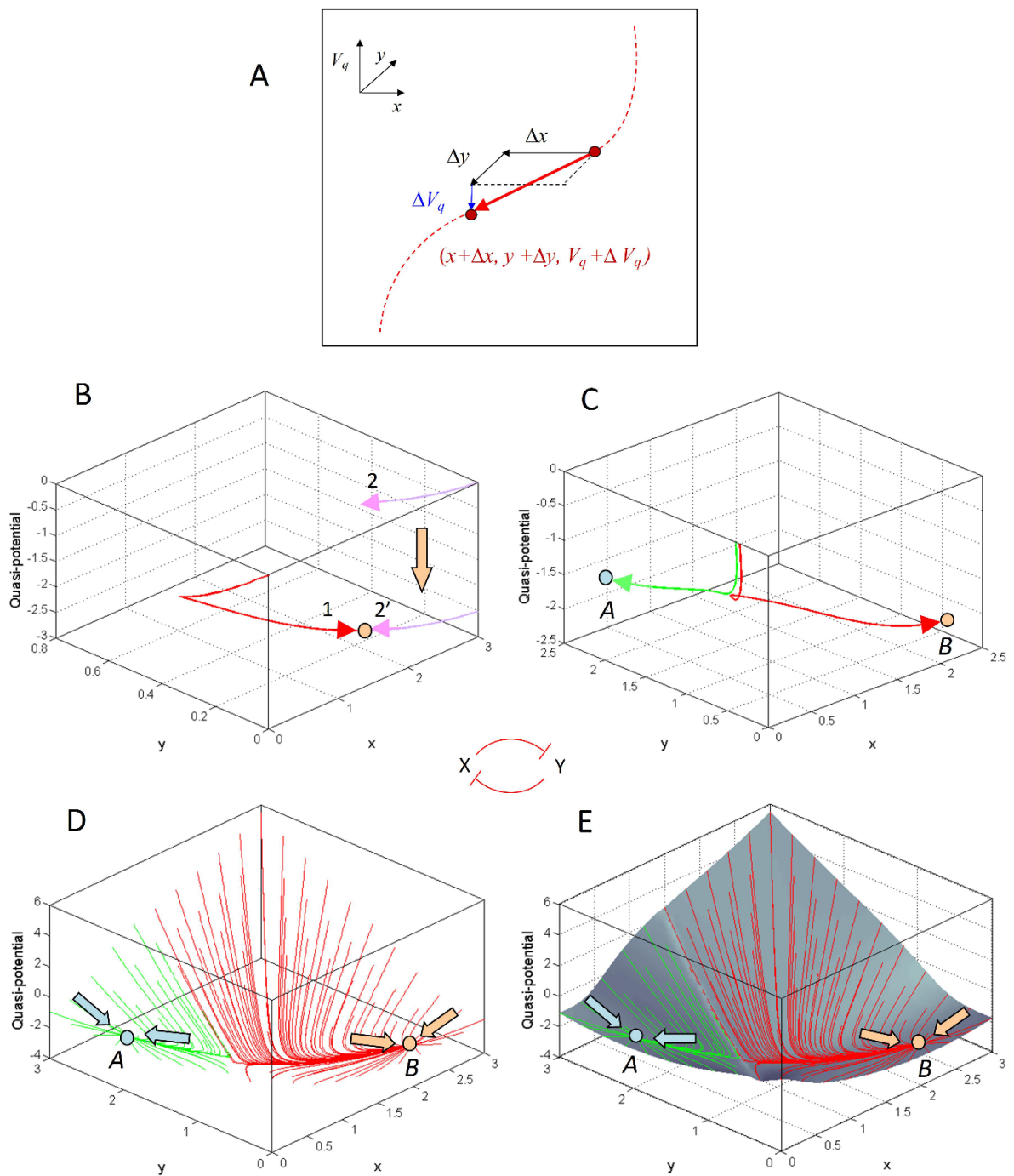
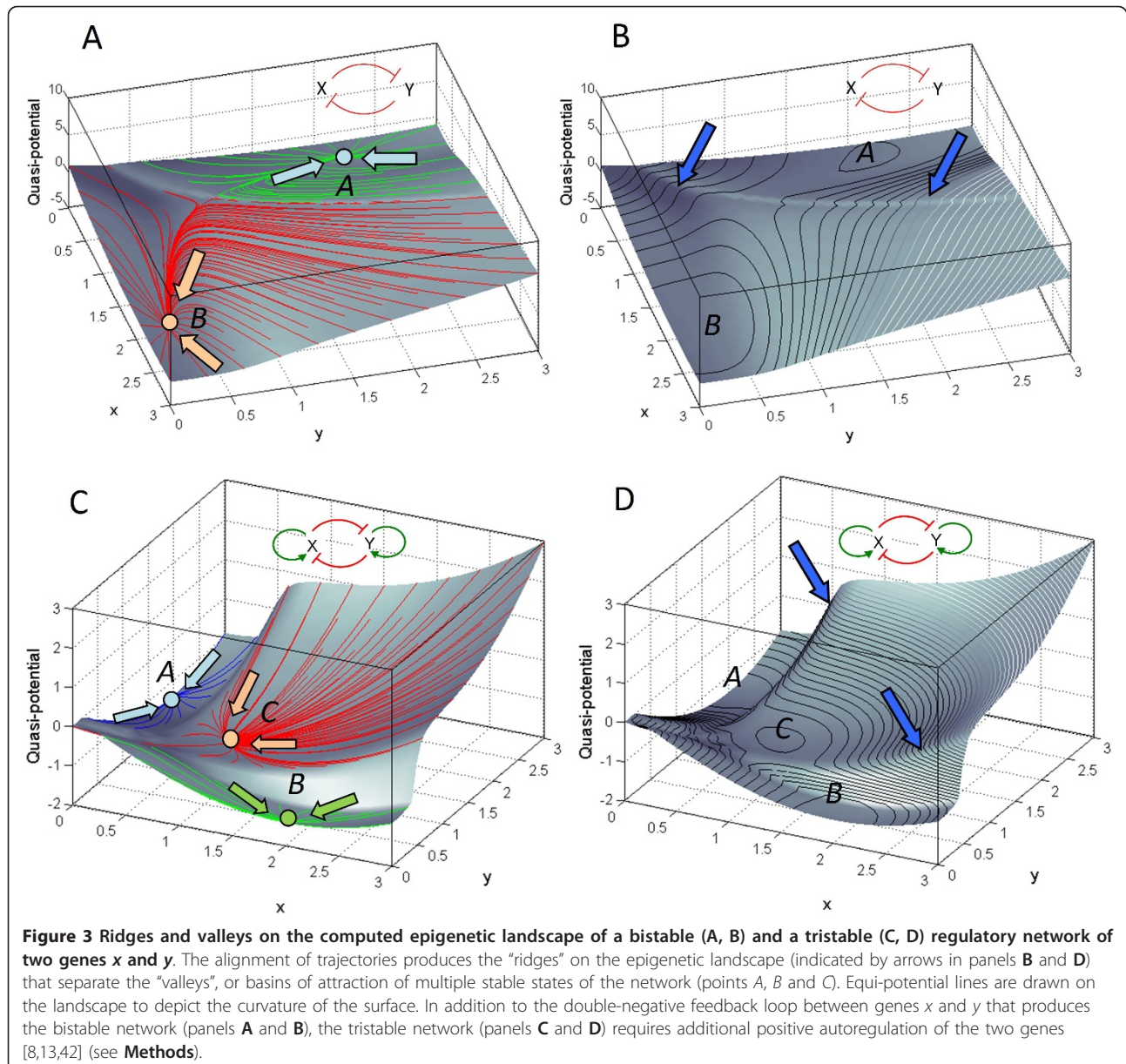


**Figure 2** Computing the epigenetic landscape for a bistable switch based on a double-negative feedback circuit of two genes  $x$  and  $y$ . **(A)** Paths followed by a simulated cell on the epigenetic landscape are obtained by integrating the change in quasi-potential  $\Delta V_q$  (Eq. 4 in text) along a trajectory as a function of time.  $(x+\Delta x)$  and  $(y+\Delta y)$  give the new position at each step along the trajectory in  $x$ - $y$  phase space, while  $(V_q + \Delta V_q)$  gives the new elevation on the quasi-potential surface. The initial value of the quasi-potential at the start of any individual trajectory is arbitrarily set to zero. **(B)** Two trajectories (1 and 2) that converge to the same attractor on the  $x$ - $y$  phase plane are aligned vertically so that both trajectories also converge to the same quasi-potential level. **(C)** Two trajectories that originate at adjacent points on the phase plane but converge to different attractors  $A$  and  $B$  are aligned vertically so that the initial quasi-potential levels of the two trajectories are equal. **(D)** Multiple trajectories starting from different points on the  $x$ - $y$  phase plane are then aligned as described in panels **B** and **C**. To identify distinct basins of attraction, trajectories are shown colored according to the attractor to which they converge (arrows). This two-gene double-negative feedback circuit produces a bistable system with two attractors  $A$  and  $B$ . **(E)** Finally, interpolation among multiple trajectories aligned across the phase plane produces the epigenetic landscape.



states - two of which represent alternative differentiated cell lineages, while the third state depicts the common progenitor cell of the two lineages [8,13,42].

### Quantitative interpretation of the quasi-potential landscape

To establish that the “elevation” of the computed landscape at a given location in  $x$ - $y$  phase space correlates inversely to the probability of occurrence of the corresponding network state, we used stochastic simulations [43] of the underlying gene network. These simulations, which take into account fluctuations in gene expression levels [44] in a population of simulated “cells” (multiple instances of the gene network), showed that the “valleys”

of low elevation on the computed epigenetic landscape correspond to stable cellular states, with “deeper” valleys associated with higher probability of occupancy than shallower valleys (Figure 4A-D). On the other hand, the “ridges” separating the valleys represent barriers to stochastic transitions between multiple steady states. Varying the parameters in the network model to increase the height of the ridges relative to the valleys dramatically reduced the probability of transitions between the steady states (Figure 5), even though there was no appreciable change in the relative distance between the steady states on the  $x$ - $y$  phase plane (Figure 4A-D, right panels).

The “third dimension” (elevation) of the landscape represented by the quasi-potential, although directly

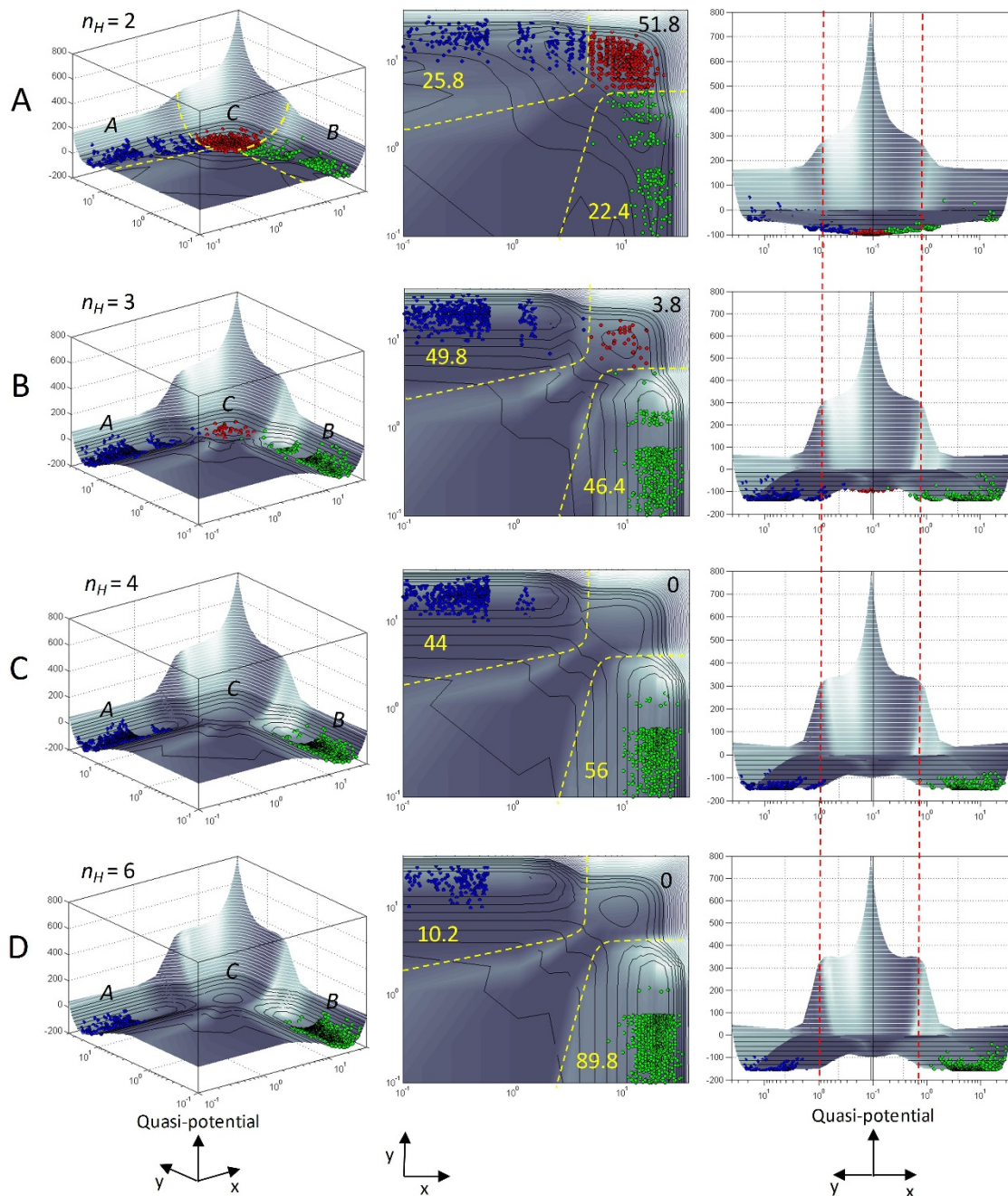


**Figure 4** Valleys on the computed epigenetic landscape represent high-occupancy stable steady states, while ridges represent barriers to stochastic transitions between those stable states. For the tristable two-gene system, increasing the Hill coefficient  $n_H$ , which represents the degree of ultrasensitivity in autoregulation and mutual inhibition of the two genes (see **Methods**), makes the ridges (barriers) higher and steeper relative to the valleys (attractors). Higher ridges reduce the probability of stochastic switching among adjacent attractors. **(A)**  $n_H = 2$ ; **(B)**  $n_H = 3$ ; **(C)**  $n_H = 4$ ; **(D)**  $n_H = 10$ . **Left Panels:** Colored circles represent a population of 1000 stochastically simulated “cells” residing in the three stable steady states A (blue), B (green) and C (red). States A and B represent two alternative differentiated cell fates, and state C their common progenitor state [8,13,42]. All simulations were started from state B as the initial condition, and run to time  $t = 10,000$  (dimensionless units). As the ridges separating the steady states grow higher, fewer cells are able to escape state B for states A and C through stochastic fluctuations. **Middle Panels:** Projections of the epigenetic landscape onto the  $x$ - $y$  phase plane. Numbers refer to the percentage of simulated cells residing in the respective steady states. Dashed yellow lines show boundaries between the basins of attraction of the steady states. **Right Panels:** An alternative view of the epigenetic landscape. The vertical dashed red lines are guides to the eye to show that the relative distance between the steady states on the  $x$ - $y$  phase plane does not change appreciably even as the Hill coefficient  $n_H$  is increased from 2 to 6. The change in relative occupancy of the attractors can therefore be attributed to the increased height and steepness of the barriers separating them.

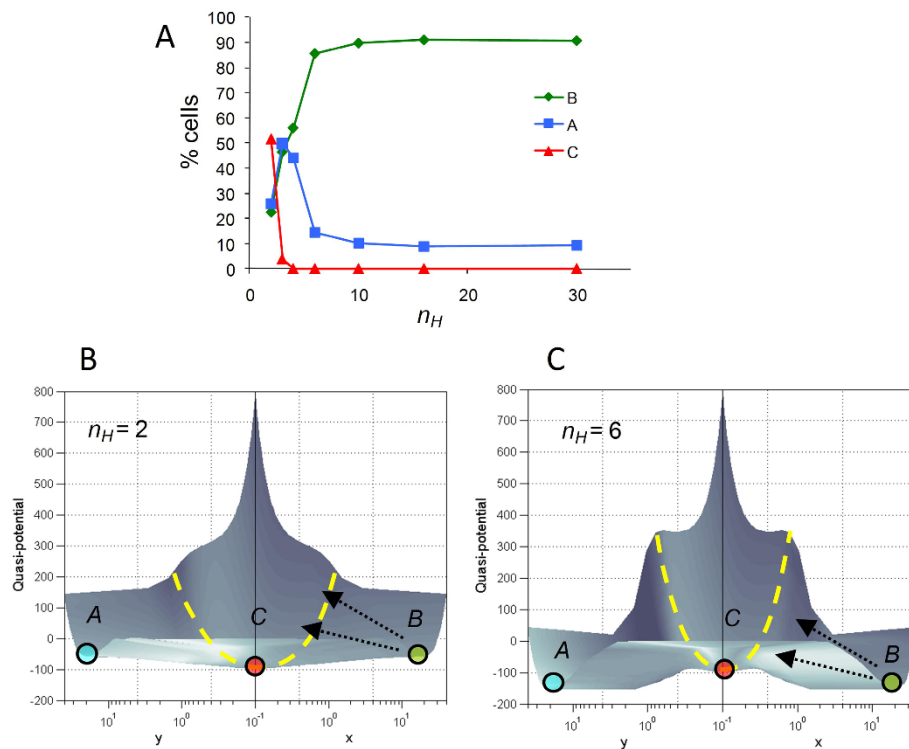


**Figure 5 Height and steepness of barriers affects stochastic occupancy of stable states. (A)** Percentage of stochastically simulated cells in the three attractors A, B and C in the tristable two-gene system at time  $t = 10,000$  for a range of values of the Hill coefficient  $n_H$ . All simulations were started from state B as the initial condition, and run to time  $t = 10,000$  (dimensionless units). **(B, C)** With increasing  $n_H$ , the height and steepness of the ridges relative to the valleys is increased, making stochastic transitions (arrows) from state B to state C, and thereafter to state A, less likely. (At longer time scales, where the distribution of the cell population among various attractors approaches an equilibrium, the percentage of cells in each attractor correlates simply to the relative depth of the attractor: see Figure S1, Additional File 1.) **(B)**  $n_H = 2$ ; **(C)**  $n_H = 6$ .

derived from the dynamic rate equations without any additional information, thus yields an interpretation of cellular stability not immediately apparent from two-dimensional phase portrait analysis. The analysis above supports the contention that the length of the “least action trajectory” along the contours of the epigenetic landscape is more important in predicting transitions between alternative cellular states than the simple “aerial distance” in state space [13]. It is also interesting to note that the contours of the quantitatively mapped epigenetic landscape act as a constraint on the extent of stochastic fluctuations in protein levels, with simulated cells “smeared out” on the surface of a shallower basin (Figure 4A, middle panel) compared to a tighter distribution of cells on a deeper valley (Figure 4D, middle panel).

These results suggest that calculating the relative heights of the ridges and valleys on the computed epigenetic landscape of a multi-gene system can help predict the probability of trans-differentiation from one cell lineage to another, or de-differentiation of a particular cell type to its progenitor state. Current efforts to reprogram cell fate with potential application in regenerative

medicine suffer from a low rate of successful reprogramming [36] and a trial-and-error approach to choice of a reprogramming strategy [13]. Computing the epigenetic landscape for the critical gene interactions regulating the transition between two cellular states may indicate particular genetic manipulations that would lower the barriers separating the two states, thereby increasing the efficiency of the reprogramming process. It can also help characterize the relative ease or difficulty of alternative routes of cell fate transition [7,9,36]. For instance, comparison of the elevation of the barriers separating two terminally-differentiated cell lineages on the epigenetic landscape might suggest that de-differentiation of cells of one lineage to the common progenitor cell of the two lineages followed by redirection to the second lineage would lead to more efficient reprogramming than direct trans-differentiation (Figure S2, Additional File 1).

#### A dynamic landscape

The computed epigenetic landscape derived above should not be interpreted as a static surface [45]. Alterations in gene interactions in course of development or



experimental manipulation will change the shape of the landscape, in turn altering the stability of individual steady states or creating novel steady states. For instance, increasing the basal expression of one gene in the tristable gene network sharply lowers the elevation of the corresponding attractor state relative to the other attractors (Figure 6A, B). As a result, cells located in the shallower attractor are destabilized and “roll into” the valley representing the deeper, more stable attractor state. This may explain the phenomenon of trans-differentiation of cells of one lineage into another by forced expression of a gene regulating the second lineage or by conditional deletion of a gene required for the first lineage [29,30].

Interestingly, this flexibility of the quasi-potential surface under gene manipulation gives a quantitative interpretation of the revised image of the epigenetic landscape proposed by Waddington (Figure S3, Additional File 1), which showed an array of pegs representing genes, holding up a sheet of fabric (the landscape) through a network of guy ropes (gene interactions) - meant to convey the idea that “the modelling of the epigenetic landscape ... is controlled by the pull of these numerous guy-ropes which are ultimately anchored to the genes [5]”. Similar changes in the shape of the epigenetic landscape may also be brought about by external signals - for example endogenous cytokines or environmental chemicals - which by transiently altering the landscape could have an instructive effect on cell fate choice.

## Conclusions

In this work, we have defined a deterministic quasi-potential that is minimized along a temporal trajectory followed by a gene network, and used it to quantitatively derive the corresponding epigenetic landscape. A gene

network not being a mechanical system, this quasi-potential should not be confused with a potential energy function. It is rather a Liapunov function of the dynamical system represented by the gene network, along which trajectories flow monotonically “downhill” towards the steady states of the network [41]. Other investigators have used a term analogous to the quasi-potential difference  $\Delta V_q$  in Eq. 4 to calculate the “energy landscape” for concentrations of one component in a gene network [46,47]. Here we have used the concept of alignment of multiple trajectories to interpolate the epigenetic landscape of a two-variable system.

This novel and simple process for deriving the surface of the landscape from a path-integral quasi-potential is not restricted to two-gene systems. While the landscape cannot be visually rendered for circuits with more than two genes, the rates of transition across the potential barriers between multiple steady states in the system can still be computed to predict optimum routes of cell fate reprogramming.

However, many binary branching points in development, particularly in blood cell lineage specification, are governed by mutual antagonism of only two transcription factors associated with alternative lineage choices [37]. Mapping the epigenetic landscape of pairs of such cross-inhibitory “master regulators” should therefore be of particular interest in understanding both normal development and induced cell fate reprogramming, and can be greatly aided by detailed quantitative characterization of the interactions between these regulators.

## Methods

### Bistable network model

To illustrate the derivation of the epigenetic landscape, we used a simplified mathematical model of a bistable

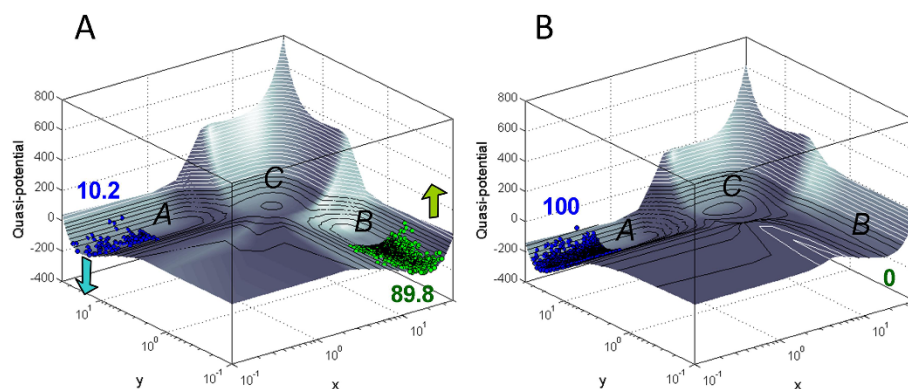


**Figure 6** The shape of the computed epigenetic landscape can be altered by modifying gene interaction parameters. When basal expression  $B_y$  of gene  $y$  in the tristable two-gene system (see **Methods**) is increased from  $B_y = 0$  (A) to  $B_y = 4$  (B) (dimensionless units), attractor A on the landscape is “lowered” relative to attractor B, causing cells to “roll into” the more stable state A from the destabilized state B. Numbers on the figure refer to the percentage of stochastically simulated cells in the respective attractors. All simulations were started from state B as the initial condition, and run to time  $t = 10,000$ . Hill coefficient  $n_H = 10$  in both figures.

network of two genes,  $x$  and  $y$ , that suppress each other to form a double-negative feedback loop. The dynamics of the model are described by the two rate equations:

$$\frac{dx}{dt} = B_X + \frac{fold_{YX} \cdot K_{DYX}^{n_H}}{K_{DYX}^{n_H} + \gamma^{n_H}} - deg_X \cdot x \quad (6)$$

$$\frac{dy}{dt} = B_Y + \frac{fold_{XY} \cdot K_{DXY}^{n_H}}{K_{DXY}^{n_H} + x^{n_H}} - deg_Y \cdot y \quad (7)$$

where variables  $x$  and  $y$  represent the concentrations of the two gene products, and parameters  $B_X$  and  $B_Y$  denote the basal (constitutive) expression rates of genes  $x$  and  $y$ , respectively. The parameters  $fold_{YX}$  and  $fold_{XY}$  represent the rate constants, and  $K_{DYX}$  and  $K_{DXY}$  the effective affinity constants, for the suppressive effects of gene  $y$  on gene  $x$ , and of gene  $x$  on gene  $y$ , respectively. The mutual suppression of the two genes is quantified by the Hill-coefficient  $n_H$  (the interaction is *ultrasensitive* for values of  $n_H > 1$ ). Parameters  $deg_X$  and  $deg_Y$  represent the first-order degradation rate constants for the two gene products  $x$  and  $y$ , respectively. For this simplified model we used dimensionless parameters with the following values:  $fold_{YX} = fold_{XY} = 2$ ;  $K_{DYX} = 0.7$ ;  $K_{DXY} = 0.5$ ;  $B_X = B_Y = 0.2$ ;  $deg_X = deg_Y = 1$ ;  $n_H = 4$ . These values were tuned to ensure bistable switching behavior in the model.

### Tristable network model

The tristable network model consisted of two genes,  $x$  and  $y$ , that in addition to mutual suppression, induce their own expression (positive autoregulation). The dynamics of this model are described by:

$$\frac{dx}{dt} = B_X + \frac{fold_{XX} \cdot x^{n_H}}{K_{DXX}^{n_H} + x^{n_H}} + \frac{fold_{YX} \cdot K_{DYX}^{n_H}}{K_{DYX}^{n_H} + \gamma^{n_H}} - deg_X \cdot x \quad (8)$$

$$\frac{dy}{dt} = B_Y + \frac{fold_{YY} \cdot y^{n_H}}{K_{DYY}^{n_H} + y^{n_H}} + \frac{fold_{XY} \cdot K_{DXY}^{n_H}}{K_{DXY}^{n_H} + x^{n_H}} - deg_Y \cdot y \quad (9)$$

where the new parameters  $fold_{XX}$  and  $fold_{YY}$  represent the rate constants, and  $K_{DXX}$  and  $K_{DYY}$  the effective affinity constants, for the positive autoregulation of genes  $x$  and  $y$ , respectively. The default parameter values chosen to ensure three robust stable states in this model were as follows:  $fold_{XX} = fold_{YY} = fold_{YX} = fold_{XY} = 10$ ;  $K_{DXX} = K_{DYY} = K_{DYX} = K_{DXY} = 4$ ;  $B_X = B_Y = 0$ ;  $deg_X = deg_Y = 1$ ;  $n_H = 4$ . This system has been modeled previously [42,48,49] in the context of mutual inhibition of the transcription factors PU.1 and GATA1 in common myeloid progenitor (CMP) cells, which gives rise to either bipotential granulocyte/macrophage progenitor (GMP) cells or megakaryocyte/erythroid progenitor (MEP) cells.

### Integration Algorithm

To evaluate the change in the quasi-potential along each trajectory in  $x$ - $y$  phase space by numerical integration, the initial level of the quasi-potential at time  $t = 0$  at the origin of the trajectory was arbitrarily set to zero (the same initial quasi-potential level was used for all trajectories so that the drop in the quasi-potential along each trajectory could be compared and used as a basis for alignment of multiple trajectories along a basin of attraction).

Thereafter, at each time step:

- The rates  $\frac{dx}{dt}$  and  $\frac{dy}{dt}$  were updated to the current value of  $x$  and  $y$  according to Eqs. 8 and 9.
- Expression levels  $x$  and  $y$  were updated as:

$$x_{new} = x_{old} + \Delta x \quad (10)$$

$$y_{new} = y_{old} + \Delta y \quad (11)$$

where for increments in time  $\Delta t$  (fixed for a simulation to ensure convergence), the changes in  $x$  and  $y$  are given by:

$$\Delta x = \frac{dx}{dt} \cdot \Delta t \quad (12)$$

$$\Delta y = \frac{dy}{dt} \cdot \Delta t \quad (13)$$

- The quasi-potential  $V_q$  was updated as:

$$V_q^{new} = V_q^{old} + \Delta V_q \quad (14)$$

where:

$$\Delta V_q = -\frac{dx}{dt} \cdot \Delta x - \frac{dy}{dt} \cdot \Delta y \quad (15)$$

The above steps were repeated until the quasi-potential  $V_q$  converged to a minimum (decided by a pre-set tolerance). Multiple trajectories thus obtained were aligned into basins of attraction according to the process described in the main text. The quasi-potential surface was then derived by linear interpolation among the aligned trajectories.

### Software platforms used

The deterministic models were implemented and simulated on the MATLAB<sup>®</sup> (R2009a, The MathWorks, Inc., Natick, MA) platform, while the BioNetS program [50], based on the Gillespie algorithm [51,52], was used for

stochastic simulations. All graphics were rendered on MATLAB<sup>®</sup>.

### Visualization of stochastic simulation results

The stochastically simulated “cells” (i.e. individual realizations of the stochastic network model) were overlaid on the quasi-potential surface at the  $x$  and  $y$  values predicted for each cell. Since stochastic simulations yield integral values, we added a small random “deviation” term [= ( $rand * 0.5$ ) where  $rand$  is a MATLAB<sup>®</sup> function that draws pseudorandom values from the standard uniform distribution on the open interval (0,1)] to each simulated  $x$  and  $y$  value to visualize multiple cells situated at the same point in  $x$ - $y$  phase space. The appropriate “elevation” for each cell on the quasi-potential surface was calculated by linear interpolation between the two points on the deterministic trajectories “closest to” the location of the cell in  $x$ - $y$  phase space. Source code for the model in MATLAB<sup>®</sup> format is appended in Additional File 2.

### Additional material

**Additional file 1: Supplementary Figures.** This file includes additional figures to supplement the text.

**Additional file 2: Supplementary Model Code.** This file lists the source code in MATLAB<sup>®</sup> format for the computational algorithm used to derive the epigenetic landscape.

### Acknowledgements

We thank J. D. Schroeter, C. Woods, R. B. Conolly, H. J. Clewell III, J.E. Trosko, M. Thattai, J. M. Haugh and B. Howell for critical discussions and reading of the manuscript. This work was supported by the Superfund Research Program of the U.S. National Institute of Environmental Health Sciences, and by the American Chemistry Council.

### Authors' contributions

SB designed the study, constructed the computational model and performed computer simulations, and wrote the paper. QZ participated in study design. QZ and MEA discussed the results and commented on the manuscript. All authors read and approved the final manuscript.

Received: 17 February 2011 Accepted: 27 May 2011

Published: 27 May 2011

### References

- Gilbert S: Epigenetic landscaping: Waddington's use of cell fate bifurcation diagrams. *Biology and Philosophy* 1991, **6**(2):135-154.
- Slack JMW: Conrad Hal Waddington: the last renaissance biologist? *Nat Rev Genet* 2002, **3**(11):889-895.
- Waddington CH: An introduction to modern genetics. London: George Allen & Unwin; 1939.
- Waddington CH: Organisers and Genes. Cambridge, UK: Cambridge University Press; 1940.
- Waddington CH: The Strategy of the Genes. London: George Allen & Unwin; 1957.
- Kauffman SA: Metabolic Stability and Epigenesis in Randomly Constructed Genetic Nets. *J Theor Biol* 1969, **22**(3):437-467.
- Enver T, Pera M, Peterson C, Andrews PW: Stem Cell States, Fates, and the Rules of Attraction. *Cell Stem Cell* 2009, **4**(5):387-397.
- Huang S: Reprogramming cell fates: reconciling rarity with robustness. *Bioessays* 2009, **31**(5):546-560.
- MacArthur BD, Ma'ayan A, Lemischka IR: Systems biology of stem cell fate and cellular reprogramming. *Nat Rev Mol Cell Biol* 2009, **10**(10):672-681.
- Thom R: Structural Stability and Morphogenesis. Reading, MA: W. A. Benjamin, Inc; 1976.
- Thom R: An Inventory of Waddingtonian Concepts. In *Theoretical Biology: Epigenetic and Evolutionary Order from Complex Systems*. Edited by: Goodwin B, Saunders P. Edinburgh: Edinburgh University Press; 1989:1-7.
- Wang J, Xu L, Wang E, Huang S: The Potential Landscape of Genetic Circuits Imposes the Arrow of Time in Stem Cell Differentiation. *Biophys J* 2010, **99**(1):29-39.
- Zhou JX, Huang S: Understanding gene circuits at cell-fate branch points for rational cell reprogramming. *Trends Genet* 2011, **27**(2):55-62.
- Kim KY, Wang J: Potential energy landscape and robustness of a gene regulatory network: Toggle switch. *PLoS Comput Biol* 2007, **3**(3):565-577.
- Cao Y, Liang J: Optimal enumeration of state space of finitely buffered stochastic molecular networks and exact computation of steady state landscape probability. *BMC Syst Biol* 2008, **2**.
- Zhu XM, Yin L, Hood L, Ao P: Robustness, stability and efficiency of phage  $\lambda$  genetic switch: Dynamical structure analysis. *J Bioinform Comput Biol* 2004, **2**(4):785-817.
- Zhu XM, Yin L, Hood L, Ao P: Calculating biological behaviors of epigenetic states in the phage  $\lambda$  life cycle. *Funct Integr Genomics* 2004, **4**(3):188-195.
- Lapidus S, Han B, Wang J: Intrinsic noise, dissipation cost, and robustness of cellular networks: The underlying energy landscape of MAPK signal transduction. *Proc Natl Acad Sci USA* 2008, **105**(16):6039-6044.
- Wang J, Xu L, Wang EK: Potential landscape and flux framework of nonequilibrium networks: Robustness, dissipation, and coherence of biochemical oscillations. *Proc Natl Acad Sci USA* 2008, **105**(34):12271-12276.
- Li C, Wang E, Wang J: Potential Landscape and Probabilistic Flux of a Predator Prey Network. *PLoS ONE* 2011, **6**(3):e17888.
- Takahashi K, Yamanaka S: Induction of pluripotent stem cells from mouse embryonic and adult fibroblast cultures by defined factors. *Cell* 2006, **126**(4):663-676.
- Takahashi K, Tanabe K, Ohnuki M, Narita M, Ichisaka T, Tomoda K, Yamanaka S: Induction of pluripotent stem cells from adult human fibroblasts by defined factors. *Cell* 2007, **131**(5):861-872.
- Wernig M, Meissner A, Foreman R, Brambrink T, Ku MC, Hochedlinger K, Bernstein BE, Jaenisch R: In vitro reprogramming of fibroblasts into a pluripotent ES-cell-like state. *Nature* 2007, **448**(7151):318-U312.
- Maherali N, Sridharan R, Xie W, Utikal J, Eminli S, Arnold K, Stadtfeld M, Yachechko R, Tchieu J, Jaenisch R, Plath K, Hochedlinger K: Directly reprogrammed fibroblasts show global epigenetic remodeling and widespread tissue contribution. *Cell Stem Cell* 2007, **1**(1):55-70.
- Yu JY, Vodyanik MA, Smuga-Otto K, Antosiewicz-Bourget J, Frane JL, Tian S, Nie J, Jonsdottir GA, Ruotti V, Stewart R, Slukvin II, Thomson JA: Induced pluripotent stem cell lines derived from human somatic cells. *Science* 2007, **318**(5858):1917-1920.
- Dimos JT, Rodolfa KT, Niakan KK, Weisenthal LM, Mitsumoto H, Chung W, Croft GF, Saphier G, Leibel R, Golland R, Wichterle H, Henderson CE, Eggan K: Induced pluripotent stem cells generated from patients with ALS can be differentiated into motor neurons. *Science* 2008, **321**(5893):1218-1221.
- Hanna J, Markoulaki S, Schorderet P, Carey BW, Beard C, Wernig M, Creighton MP, Steine EJ, Cassady JP, Foreman R, Lengner CJ, Dausman JA, Jaenisch R: Direct reprogramming of terminally differentiated mature B lymphocytes to pluripotency. *Cell* 2008, **133**(2):250-264.
- Shen CN, Slack JMW, Tosh D: Molecular basis of transdifferentiation of pancreas to liver. *Nat Cell Biol* 2000, **2**(12):879-887.
- Xie HF, Ye M, Feng R, Graf T: Stepwise reprogramming of B cells into macrophages. *Cell* 2004, **117**(5):663-676.
- Cobaleda C, Jochum W, Busslinger M: Conversion of mature B cells into T cells by dedifferentiation to uncommitted progenitors. *Nature* 2007, **449**(7161):473-477.
- Zhou Q, Brown J, Kanarek A, Rajagopal J, Melton DA: In vivo reprogramming of adult pancreatic exocrine cells to beta-cells. *Nature* 2008, **455**(7213):627-U630.
- Vierbuchen T, Ostermeier A, Pang ZP, Kokubu Y, Sudhof TC, Wernig M: Direct conversion of fibroblasts to functional neurons by defined factors. *Nature* 2010, **463**(7284):1035-U1050.

33. Ieda M, Fu JD, Delgado-Olguin P, Vedantham V, Hayashi Y, Bruneau BG, Srivastava D: **Direct Reprogramming of Fibroblasts into Functional Cardiomyocytes by Defined Factors.** *Cell* 2010, **142**(3):375-386.
34. Tursun B, Patel T, Kratsios P, Hobert O: **Direct conversion of *C. elegans* germ cells into specific neuron types.** *Science* 2011, **331**(6015):304-308.
35. Zhou Q, Melton DA: **Extreme Makeover: Converting One Cell into Another.** *Cell Stem Cell* 2008, **3**(4):382-388.
36. Yamanaka S: **Elite and stochastic models for induced pluripotent stem cell generation.** *Nature* 2009, **460**(7251):49-52.
37. Graf T, Enver T: **Forcing cells to change lineages.** *Nature* 2009, **462**(7273):587-594.
38. Huang S: **Non-genetic heterogeneity of cells in development: more than just noise.** *Development* 2009, **136**(23):3853-3862.
39. Hochedlinger K, Plath K: **Epigenetic reprogramming and induced pluripotency.** *Development* 2009, **136**(4):509-523.
40. Gardner TS, Cantor CR, Collins JJ: **Construction of a genetic toggle switch in *Escherichia coli*.** *Nature* 2000, **403**(6767):339-342.
41. Strogatz S: **Nonlinear Dynamics and Chaos: With Applications to Physics, Biology, Chemistry, and Engineering (Studies in Nonlinearity).** Cambridge, MA: Perseus Books Group; 2001.
42. Huang S, Guo YP, May G, Enver T: **Bifurcation dynamics in lineage-commitment in bipotent progenitor cells.** *Dev Biol* 2007, **305**(2):695-713.
43. Wilkinson DJ: **Stochastic modelling for quantitative description of heterogeneous biological systems.** *Nat Rev Genet* 2009, **10**(2):122-133.
44. Kaern M, Elston TC, Blake WJ, Collins JJ: **Stochasticity in gene expression: From theories to phenotypes.** *Nat Rev Genet* 2005, **6**(6):451-464.
45. Roeder I, Radtke F: **Stem cell biology meets systems biology.** *Development* 2009, **136**(21):3525-3530.
46. Hasty J, Pradines J, Dolnik M, Collins JJ: **Noise-based switches and amplifiers for gene expression.** *Proc Natl Acad Sci USA* 2000, **97**(5):2075-2080.
47. Acar M, Becskei A, van Oudenaarden A: **Enhancement of cellular memory by reducing stochastic transitions.** *Nature* 2005, **435**(7039):228-232.
48. Roeder I, Glauche I: **Towards an understanding of lineage specification in hematopoietic stem cells: A mathematical model for the interaction of transcription factors GATA-1 and PU.1.** *J Theor Biol* 2006, **241**(4):852-865.
49. Chickarmane V, Enver T, Peterson C: **Computational Modeling of the Hematopoietic Erythroid-Myeloid Switch Reveals Insights into Cooperativity, Priming, and Irreversibility.** *PLoS Comput Biol* 2009, **5**(1): e1000268.
50. Adalsteinsson D, McMillen D, Elston TC: **Biochemical Network Stochastic Simulator (BioNetS): software for stochastic modeling of biochemical networks.** *BMC Bioinformatics* 2004, **5**:24.
51. Gillespie DT: **A general method for numerically simulating the stochastic time evolution of coupled chemical reactions.** *Journal of Computational Physics* 1976, **22**(4):403-434.
52. Gillespie DT: **Exact Stochastic Simulation of Coupled Chemical-Reactions.** *J Phys Chem* 1977, **81**(25):2340-2361.

doi:10.1186/1752-0509-5-85

**Cite this article as:** Bhattacharya et al.: A deterministic map of Waddington's epigenetic landscape for cell fate specification. *BMC Systems Biology* 2011 **5**:85.

**Submit your next manuscript to BioMed Central and take full advantage of:**

- Convenient online submission
- Thorough peer review
- No space constraints or color figure charges
- Immediate publication on acceptance
- Inclusion in PubMed, CAS, Scopus and Google Scholar
- Research which is freely available for redistribution

Submit your manuscript at  
www.biomedcentral.com/submit

